nature neuroscience

β-amyloid disrupts human NREM slow waves and related hippocampus-dependent memory consolidation

Bryce A Mander[1], Shawn M Marks[2], Jacob W Vogel[2], Vikram Rao[1], Brandon Lu[3], Jared M Saletin[1], Sonia Ancoli-Israel[4], William J Jagust[2,5] & Matthew P Walker[1,2]

Independent evidence associates β-amyloid pathology with both non-rapid eye movement (NREM) sleep disruption and memory impairment in older adults. However, whether the influence of β-amyloid pathology on hippocampus-dependent memory is, in part, driven by impairments of NREM slow wave activity (SWA) and associated overnight memory consolidation is unknown. Here we show that β-amyloid burden in medial prefrontal cortex (mPFC) correlates significantly with the severity of impairment in NREM SWA generation. Moreover, reduced NREM SWA generation was further associated with impaired overnight memory consolidation and impoverished hippocampal-neocortical memory transformation. Furthermore, structural equation models revealed that the association between mPFC β-amyloid pathology and impaired hippocampus-dependent memory consolidation was not direct, but instead statistically depended on the intermediary factor of diminished NREM SWA. By linking β-amyloid pathology with impaired NREM SWA, these data implicate sleep disruption as a mechanistic pathway through which β-amyloid pathology may contribute to hippocampus-dependent cognitive decline in the elderly.

Cognitive decline is a problematic and disabling consequence of aging, with impairments in hippocampus-dependent memory being one of the most debilitating symptoms[1–4]. The accumulation of cortical β-amyloid (Aβ) and subcortical tau proteins are leading candidate mechanisms underlying hippocampus-dependent memory impairment in aging and Alzheimer's disease[2–5]. While tau pathology predominantly accumulates initially in medial temporal lobe structures, including the hippocampus[3,5], β-amyloid pathology predominates in cortex, with the earliest deposition including cortical regions such as the mPFC[2,4]. Evidence implicates both pathologies in memory failure in even healthy older adults[3,5,6]. Though tau pathology appears to exert its influence on memory through direct degeneration of hippocampal synapses[5], the mechanisms through which Aβ compromises hippocampus-dependent memory remain unclear. Aβ does not aggregate substantively within the hippocampus[2,3], but has been associated with memory through its effects on hippocampal-neocortical network structure, function and connectivity,[6,7] and through its association with hippocampal tau pathology[5]. However, the direct influence of Aβ and tau neuropathology explains only a moderate proportion of the variance in age-related cognitive decline[1]. It therefore remains possible that Aβ pathology also influences hippocampus-dependent memory indirectly, through other pathways that impact memory-relevant hippocampal-neocortical functioning.

One pathway through which cortical Aβ may trigger hippocampus-dependent memory deficits is through its disruption of NREM sleep and associated SWA[8–11]. Several independent lines of evidence support this hypothesis. First, older adults exhibit marked reductions in NREM SWA, with these reductions being associated with the degree of memory impairment observed[8–13]. Second, the degree of disrupted prefrontal NREM SWA in older adults is associated not only with the degree of impaired overnight memory retention[11], but also with persistent retrieval-related hippocampal activation that reflects impoverished hippocampal-neocortical memory transformation[11]. Third, experimentally increasing NREM SWA, specifically in the slow, <1-Hz frequency range, causally enhances consolidation and thus long-term memory retention in young adults[14]. Fourth, there is strong homology between source generators of NREM slow wave oscillations, which predominate in medial prefrontal cortex (mPFC)[15], and the cortical regions where Aβ preferentially aggregates in cognitively normal older adults and in Alzheimer's disease patients[2,15]. Fifth, age-related NREM slow wave sleep disruption is exacerbated at an early stage in the progression of Alzheimer's disease and mild cognitive impairment, both conditions expressing elevated Aβ burden[13,16,17]. Further, the severity of NREM sleep disruption in these patient groups predicts the severity of observed memory impairment[13,18]. Finally, interstitial Aβ levels in humans and rodents rise and fall with the brain states of wakefulness and NREM sleep, respectively. Additionally, mice overexpressing Aβ protein demonstrate shorter NREM sleep duration and greater NREM sleep fragmentation[19,20], with direct manipulations of sleep and Aβ production in rodent models establishing bidirectional relationships between these factors[19–21]. Moreover, cortical Aβ burden correlates with subjective reports of reduced sleep duration and diminished sleep quality in older adult humans[22].

[1]Sleep and Neuroimaging Laboratory, University of California, Berkeley, California, USA. [2]Helen Wills Neuroscience Institute, University of California, Berkeley, California, USA. [3]Division of Pulmonary and Critical Care Medicine, California Pacific Medical Center, San Francisco, California, USA. [4]Department of Psychiatry, University of California, San Diego, La Jolla, California, USA. [5]Life Sciences Division, Lawrence Berkeley National Laboratory, Berkeley, California, USA. Correspondence should be addressed to B.A.M. (bamander@berkeley.edu) or M.P.W. (mpwalker@berkeley.edu).

Received 25 February; accepted 30 April; published online 1 June 2015; doi:10.1038/nn.4035

These data generate the untested hypothesis that the severity of local Aβ accumulation in mPFC is associated with diminished NREM SWA that, in turn, further correlates with the extent of impaired overnight hippocampus-dependent memory consolidation in older adults. Here, we test this hypothesis by combining [^{11}C]PIB (Pittsburgh compound B) positron emission tomography (PET) scanning, offering *in vivo* estimates of regional Aβ burden, with a night of sleep electroencephalography (EEG) and a behavioral and functional magnetic resonance imaging (fMRI) test of sleep-dependent memory consolidation. First, we hypothesized that the accumulation of Aβ in the mPFC would be associated with disrupted memory retention through its association with NREM SWA. Specifically, we predicted that mPFC Aβ burden would significantly correlate with severity of disrupted NREM SWA, particularly in the 0.6–1 Hz range known to promote memory consolidation[14,23]. Second, we posited that such disruption in NREM SWA would correlate with the degree of impaired overnight memory retention and persistent reliance (rather than progressive independence) of post-sleep retrieval on hippocampal activity. Third, bridging these relationships, we predicted that the association between mPFC β-amyloid pathology and impaired hippocampus-dependent memory would not be direct (that is, independent of sleep), but instead significantly accounted for by the intermediary factor of diminished NREM SWA.

RESULTS

Twenty-six cognitively normal older adults (**Table 1**) received a PIB-PET scan and then performed a sleep-dependent episodic associative (word-pair) task before and after a night of polysomnographically recorded sleep, with next-day retrieval-related brain activity measured using functional MRI (fMRI) (see Online Methods). For the memory test, all participants were initially trained to criterion on a set of word pairs in the evening, before sleep, followed by two separate recognition memory tests. The first ('short-delay') recognition memory test occurred 10 min after the initial study session, when a subset of the studied word pairs were tested. Following the short-delay recognition test, participants were given the in-laboratory, 8-h sleep recording period in accordance with habitual sleep-wake habits. The next morning, participants performed the second ('long-delay'), post-sleep recognition test during an fMRI scanning session, when the remaining subset of originally studied word pairs was tested. Functional MRI scanning was employed to assess post-sleep retrieval-related activity, focused a priori on the hippocampus[24]. The measure of overnight memory retention was calculated by subtracting short-delay recognition performance from long-delay recognition performance[8,11].

β-amyloid and NREM SWA

Given our hypothesized associations between Aβ pathology, NREM slow wave sleep and episodic memory retention, we first examined associations between mPFC NREM SWA (mean at midline frontal and central (FZ and CZ) EEG derivations) and Aβ pathology (the latter indexed using PIB-PET distribution volume ratios (DVRs)) (**Fig. 1a–d**). Because of the causal role of lower frequency (<1-Hz) NREM SWA in memory consolidation[14,23], we first examined the impact of Aβ on NREM SWA by frequency. A two-way, repeated-measures analysis of covariance (ANCOVA), with frequency (0.6–1 Hz or 1–4 Hz) as a within-subjects factor and mPFC PIB as a between-subjects covariate, revealed a significant frequency × mPFC PIB interaction ($P = 0.032$; **Fig. 2a**). Specifically, greater mPFC PIB DVR was associated with lower NREM SWA in the 0.6–1 Hz range (parameter estimate $t = -2.29$, $P = 0.031$), but not in the faster frequency range (1–4 Hz: parameter estimate $t = 1.85$, $P = 0.076$) over prefrontal cortex.

Table 1 Demographic and neuropsychological measures (mean ± s.d.)

Variable	Subjects ($n = 26$)
Age (years)	75.1 ± 3.5
Sex	18 female
Education (years)	16.5 ± 2.2
MMSE	29.5 ± 1.0
PIB index	1.13 ± 0.21
mPFC PIB	1.16 ± 0.25
Occipital lobe PIB	1.10 ± 0.08
Temporal lobe PIB	1.07 ± 0.18
Parietal lobe PIB	1.15 ± 0.19
dlPFC PIB	1.15 ± 0.26
Mean bedtime	22:55 ± 1:20
Mean wake time	7:20 ± 1:15
Mean prestudy time in bed (h)	8.42 ± 0.73
Mean prestudy sleep time (h)	7.24 ± 0.91
Mean prestudy sleep latency (min)	38.5 ± 45.3
Mean prestudy sleep efficiency (%)	86.2 ± 10.1
Short-delay recognition (HR – FAR – LR)	0.14 ± 0.25
Long-delay recognition (HR – FAR – LR)	–0.49 ± 0.32
Memory change (long – short delay)	–0.64 ± 0.29
Neuropsychological measures	
CVLT (long-delay, no. free recalled)	10.6 ± 3.0
WMS (visual reproduction %)	71.3 ± 15.9
Trailmaking B (s)	76.0 ± 35.7
Stroop (no. correct in 60 s)	47.6 ± 13.6

MMSE, Mini Mental state exam; CVLT, California Verbal Learning Test; WMS, Wechsler Memory Scale. "No. free recalled" refers to the number of studied words freely recalled after a long delay, visual reproduction refers to recognition memory of nonverbal visual stimuli, trailmaking B refers to a test of task-switching ability and Stroop refers to a test of directed attention and cognitive inhibition.

The proportion of mPFC SWA 0.6–1 Hz was also negatively associated with mPFC PIB ($r = -0.45$, $P = 0.020$; **Fig. 2b**). Moreover, the relationship between mPFC PIB and proportion of mPFC NREM SWA 0.6–1 Hz persisted when accounting for the non-normal distribution of PIB DVRs by using nonparametric analysis (Kendall's $\tau = -0.30$, $P = 0.035$). Indicating specificity, no other significant NREM sleep associations were detected (**Supplementary Table 1**).

These Aβ pathology associations remained significant when accounting for the factors of age, mPFC gray matter volume (optimized voxel-based morphometry measure) and sex within the same statistical model ($P = 0.026$ for mPFC PIB, yet $P = 0.753$ for age, $P = 0.781$ for gray matter and $P = 0.660$ for sex). This last nonsignificant effect should be appreciated cautiously, as an exploration of sex differences was not part of the primary hypotheses and the design and power of the study was not adequate to discount potential sex-based interactions.

To address the mPFC specificity of our PIB DVR and NREM SWA 0.6–1 Hz associations, we used two-way, repeated measures ANCOVA models. In the first model, we examined whether SWA at different derivations was associated with mPFC PIB DVRs. In this model, mPFC PIB was included as a between-subjects covariate with location of proportion of NREM SWA 0.6–1 Hz (mPFC, dorsolateral PFC (dlPFC), parietal cortex, temporal cortex or occipital cortex) included as a within-subjects factor. In this model, location ($F = 24.002$, $P < 0.001$) and location × mPFC PIB DVR ($F = 2.568$, $P = 0.043$) were significant whereas mPFC PIB DVR was not ($F = 3.871$, $P = 0.061$). Parameter estimates from this model suggested that only frontal locations were significantly associated with mPFC PIB DVR, with peak significance being detected over mPFC (for mPFC, $P = 0.020$; for dlPFC, $P = 0.027$; there were nonsignificant associations for parietal $P = 0.118$, temporal $P = 0.105$ and occipital $P = 0.162$ locations). In the second ANCOVA model, the proportion of mPFC SWA 0.6–1 Hz was included as a between-subjects covariate with location of PIB DVR

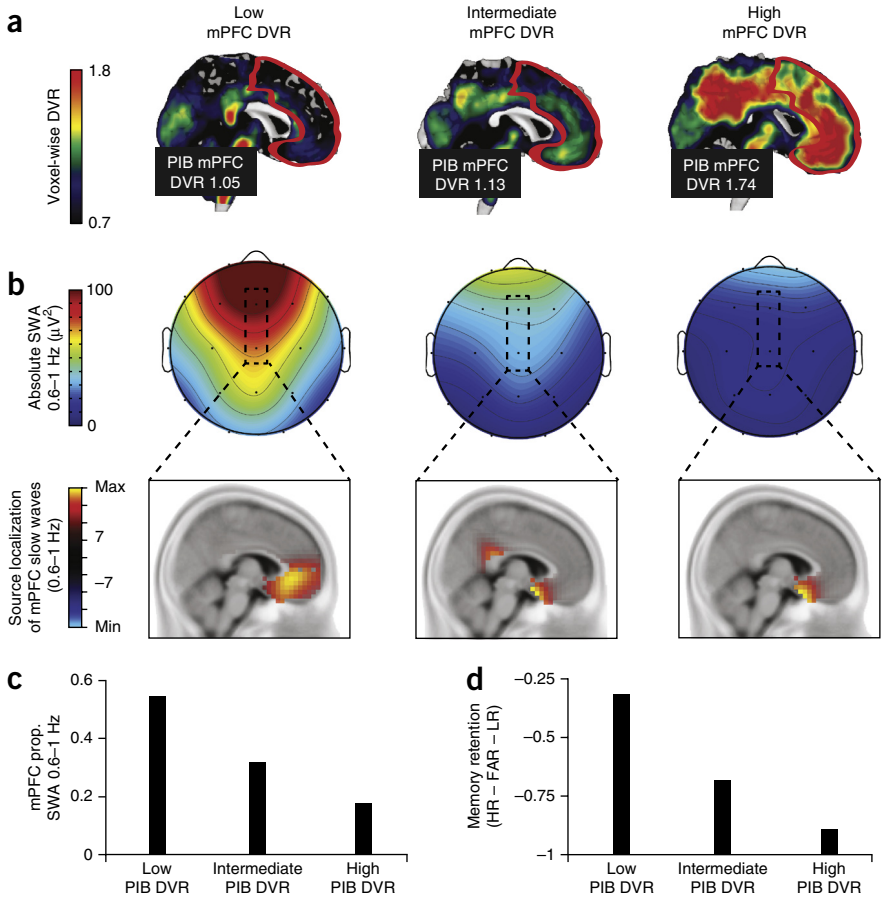

Figure 1 Aβ, NREM SWA and memory retention measures in three sample subjects. (**a**–**d**) [^{11}C]PIB-PET DVR images demonstrating Aβ deposition (**a**), NREM SWA and associated localized slow wave source (in arbitrary units) (**b**), proportion of NREM SWA 0.6–1 Hz at FZ and CZ derivations (**c**) and overnight memory retention (long-delay recognition testing – short-delay recognition testing) (**d**). Left column, a subject with low mPFC PIB DVR, middle column, intermediate mPFC PIB DVR (middle column); right column, high mPFC PIB DVR. The PIB-PET mPFC region of interest (ROI) is outlined in red (**a**) and the mPFC EEG derivations are outlined in black (**b**), with accompanying source analysis (thresholded at ±7) verifying mPFC overlap across PIB-PET and EEG ROIs (see Online Methods and **Supplementary Fig. 2**). Prop., proportion; HR – FAR – LR, hit rate to originally studied word pairs minus false alarm rate to new, unstudied words minus false alarm rate to originally studied word pairs. DVR was referenced against the whole cerebellum.

(mPFC, dlPFC, parietal cortex, temporal cortex or occipital cortex) included as a within-subjects factor. In this model, location ($F = 8.331$, $P < 0.001$) and location × proportion of mPFC SWA 0.6–1 Hz ($F = 6.219$, $P < 0.001$) were significant, whereas the proportion of mPFC SWA 0.6–1 Hz was a trend ($F = 4.084$, $P = 0.055$). Thus, parameter estimates from this model suggested that only frontal regions were significantly associated with proportion of mPFC SWA 0.6–1 Hz, with peak significance being detected over mPFC (for mPFC, $P = 0.020$; for dlPFC, $P = 0.034$; there were trends or nonsignificant associations for parietal $P = 0.072$, temporal $P = 0.162$ and occipital $P = 0.217$ cortex). Finally, mPFC PIB was not associated with the proportion of rapid eye movement (REM) delta power 0.6–1 Hz over prefrontal cortex ($r = -0.31$, $P = 0.123$; Kendall's $\tau = -0.16$, $P = 0.269$), demonstrating that the association between mPFC PIB and SWA 0.6–1 Hz was specific to NREM sleep. Further, no significant association between mPFC PIB and NREM spectral power was detected beyond the SWA range (**Supplementary Fig. 1a**). Together, these data indicate that mPFC Aβ aggregation significantly predicts the degree of NREM SWA impoverishment over mPFC in the memory-relevant 0.6–1 Hz range.

To determine whether the association between β-amyloid pathology and NREM SWA 0.6–1 Hz was driven by a reduction in the number of slow waves generated or a disruption in slow wave morphology, slow waves (SW) were detected and examined using an established algorithm[25]. As in the analysis of mPFC NREM SWA, a two-way, repeated measures ANCOVA, with frequency (0.6–1 Hz or 1–4 Hz) as a within-subjects factor and mPFC PIB as a between-subjects covariate, revealed a significant frequency × mPFC PIB interaction predicting mPFC slow wave density ($P = 0.020$; **Fig. 2c**) but not mean slow wave period ($P = 0.257$), amplitude ($P = 0.685$) or the negative slope of the slow wave ($P = 0.535$). Congruent with the measure of mPFC NREM SWA, mPFC PIB was associated with lower mPFC SW density at 0.6–1 Hz (parameter estimate $t = -2.623$, $P = 0.015$) and higher SW density at 1–4 Hz (parameter estimate $t = 2.416$, $P = 0.024$). These data suggest that the association between NREM SWA at 0.6–1 Hz and β-amyloid pathology is significantly accounted for by the reduction in the incidence of 0.6–1 Hz slow waves, rather than morphological changes in SW slope, amplitude or period.

That mPFC PIB was associated with reduced SW generation in the mPFC was explored by performing source analysis. The sLORETA (standardized low-resolution brain electromagnetic tomography) method[26] was implemented, time-locking to the negative SW peak. Source results demonstrated a peak current density located in the mPFC for the negative peak of slow waves detected at CZ and FZ (0.6–1 Hz SW source; **Fig. 1b** and **Supplementary Fig. 2**). These data support the conclusion that mPFC Aβ deposition is associated with fewer slow waves 0.6–1 Hz generated in the mPFC.

NREM SWA and hippocampus-dependent memory

Next, we sought to determine whether reduced mPFC NREM SWA 0.6–1 Hz, associated with higher mPFC β-amyloid burden, predicted impaired long-term memory retention in cognitively healthy older adults. The proportion of mPFC NREM SWA 0.6–1 Hz ($r = 0.50$, $P = 0.019$; **Fig. 2d**) positively predicted memory retention. This association remained significant when controlling for age and sex ($P = 0.022$ for mPFC NREM SWA 0.6–1 Hz, $P = 0.980$ for age, $P = 0.494$ for sex). Therefore, reductions in mPFC NREM SWA 0.6–1 Hz predicted worse overnight memory retention.

At the neural level, and consistent with the hippocampal-neocortical model of memory consolidation[27,28], the severity of impairment in NREM SWA 0.6–1 Hz was further associated with greater persistence (rather than progressive independence[11,29–31]) of post-sleep retrieval-related hippocampal activation ($r = -0.59$, $P = 0.004$; **Fig. 3a**). This association also remained significant when controlling

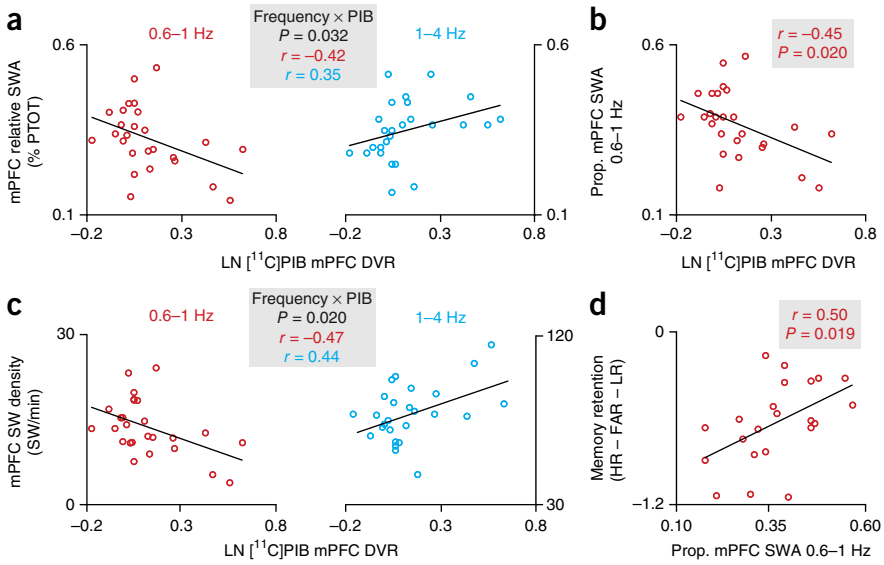

Figure 2 Associations between Aβ, NREM SWA and memory retention measures. Associations between natural logarithm–transformed, [^{11}C]PIB-PET DVR–measured mPFC Aβ deposition, mPFC relative SWA, mPFC SW density and overnight memory retention. (**a**–**d**) Interaction plots of two-way, repeated measures ANCOVAs. Aβ burden was associated with lower relative mPFC NREM SWA and SW density 0.6–1 Hz and higher mPFC NREM SWA and SW density at 1–4 Hz. Parameter estimates for each frequency bin plotted in **a** for SWA and **c** for SW density. mPFC Aβ burden was also negatively associated with proportion of mPFC NREM SWA 0.6–1 Hz (**b**). mPFC NREM SWA 0.6–1 Hz, in turn, positively predicted overnight memory retention (**d**). %PTOT, percentage of total spectral power (0.6–50 Hz); Prop., proportion; HR – FAR – LR, hit rate to originally studied word pairs minus false alarm rate to new, unstudied words minus false alarm rate to originally studied word pairs. DVR was referenced against the cerebellum.

for age and sex ($P = 0.006$ for mPFC NREM SWA 0.6–1 Hz, $P = 0.897$ for age, $P = 0.657$ for sex). Though this association was maximal in the left hippocampus, it was present bilaterally (**Supplementary Fig. 3**). No significant associations between retrieval-related HC activation and NREM spectral power were detected beyond the SWA range (**Supplementary Fig. 1b**). Implicating diminished memory consolidation in this association between NREM SWA disruption and persistent hippocampal activity, post-sleep retrieval-related activation within the hippocampus significantly predicted worse overnight memory retention ($r = –0.50$, $P = 0.017$) (**Fig. 3b**). Together, these data indicate that the severity of NREM SWA (0.6–1 Hz) impairment over mPFC is significantly associated with worse overnight memory retention and persistent reliance on the hippocampus during next-day retrieval.

Aβ, SWA and hippocampus-dependent memory consolidation

Having characterized the separate associations between mPFC Aβ pathology, NREM SWA deficits and hippocampus-dependent memory impairment, we next sought to determine the interactions between factors using path analysis[32]. Specifically, we tested the hypothesis that mPFC Aβ pathology exerted an influence on memory not directly, but indirectly, through its impairing influence on NREM SWA that compromises sleep-dependent memory consolidation. Three models were constructed (**Fig. 4a**–**c**) and compared to one another and to standard saturation and independence control models to determine the nature of these interactions. The standardized metrics used to determine these interactions were root-mean-squared residual (RMR), goodness-of-fit index (GFI) and Bayesian information criterion (BIC; see Online Methods)[33–35]. In brief, RMR values near 0 and GFI values above 0.9 are considered evidence of sufficient model fit[34]. Lower BIC values suggest better model fits, with a difference in BIC of over 10 suggesting marked differences between the models, a difference of 6–10 suggesting a strong difference and a difference of 2–6 suggesting marginal difference[35]. In the first model (**Fig. 4a**), mPFC Aβ pathology was allowed to directly predict deficits in memory retention independent of NREM SWA (proportion of mPFC NREM SWA 0.6–1 Hz) and retrieval-related hippocampal activation. In the second model (**Fig. 4b**), mPFC Aβ pathology was associated with diminished memory retention independent of NREM SWA, instead being indirectly associated through its effect on retrieval-related hippocampal activation. In the third, sleep-dependent model (**Fig. 4c**), the associated influence of mPFC Aβ pathology on impaired memory retention was not direct. Instead, the influence of mPFC Aβ pathology was indirect, through its impact on diminished NREM SWA that consequently predicted impairments in overnight memory retention and hippocampus-dependent memory transformation. Of the three, the third, sleep-dependent model provided the superior statistical fit (**Fig. 4c**). Specifically, this sleep-dependent model provided (i) the lowest RMR (RMR = 0.006, compared to 0.021 for model 1 and 0.021

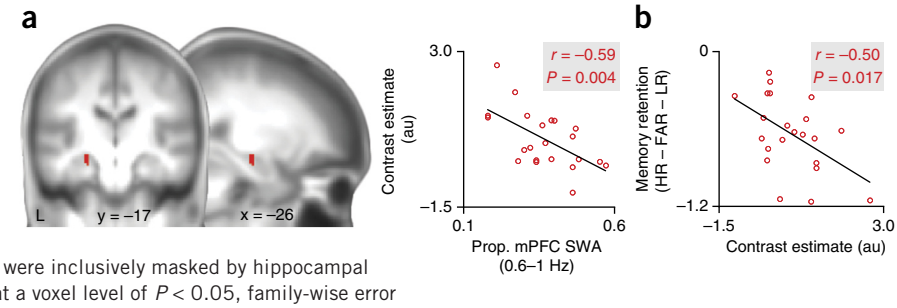

Figure 3 Associations between NREM SWA, retrieval-related hippocampus activation and memory retention. (**a**) Negative association between proportion of mPFC SWA 0.6–1 Hz and left hippocampal activation greater during successful associative episodic retrieval than correct rejection of novel words (hits – correct rejections); 8-mm-sphere ROI: [$x = –22$, $y = –14$, $z = –12$; $x = –23$, $y = –15$, $z = –16$] in Montreal Neurological Institute (MNI) template coordinates[24]. Activations were inclusively masked by hippocampal anatomy and displayed and considered significant at a voxel level of $P < 0.05$, family-wise error corrected for multiple comparisons within the a priori hippocampal region of interest. Peak effects were detected at [$x = –24$, $y = –16$, $z = –14$]. Red color brightness represents the extent of the negative association between hippocampal activation and proportion of SWA 0.6–1 Hz. (**b**) Negative association between overnight memory retention and the average contrast estimate of significant hippocampal voxels, extracted using Marsbar[46]. au, arbitrary units; Prop., proportion; HR – FAR – LR, hit rate to originally studied word pairs minus false alarm rate to new, unstudied words minus false alarm rate to originally studied word pairs.

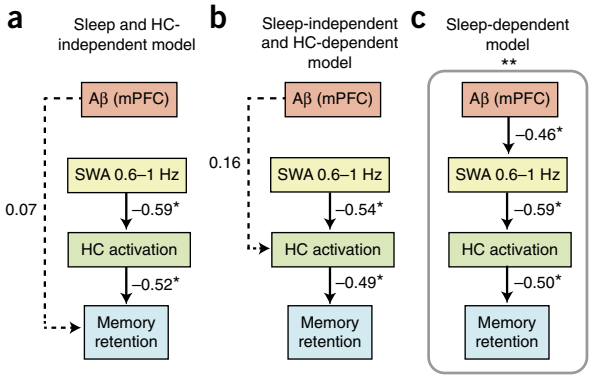

Figure 4 Path models linking Aβ, NREM SWA, retrieval-related hippocampus activation and memory retention. (**a**–**c**) Path analysis models examining the relative contributions of [^{11}C]PIB-PET DVR measured mPFC Aβ deposition, proportion of mPFC NREM SWA 0.6–1 Hz and retrieval-related hippocampal (HC) activation to overnight memory retention (long-delay recognition testing minus short-delay recognition testing) in three hypothesized models. Values represent standardized regression weights. Models were estimated, and model fits for the sleep and HC-independent model (**a**, BIC = 29.640; RMR = 0.021; GFI = 0.858), the sleep-independent and HC-dependent model (**b**, BIC = 29.131; RMR = 0.021; GFI = 0.873) and the sleep-dependent model (**c**, BIC = 24.676; RMR = 0.006; GFI = 0.931) were compared against the fits for a saturated model (BIC = 30.910; RMR = 0.000; GFI = 1.000) and an independence model (BIC = 30.747; RMR = 0.046; GFI = 0.617). *$P < 0.05$.

for model 2), (ii) the only GFI above 0.9 (GFI = 0.931, compared to 0.858 for model 1 and 0.873 for model 2) and (iii) the lowest BIC value (BIC = 24.676, compared to 29.640 for model 1 and 29.131 for model 2). Moreover, only the sleep-dependent model outperformed both the saturation (RMR = 0.000, GFI = 1.000, BIC: 30.910) and independence (RMR = 0.046, GFI = 0.617, BIC: 30.747) control models. Critically, however, while all three models demonstrated significant associations between NREM SWA 0.6–1 Hz and post-sleep retrieval-related hippocampal activation (all $P < 0.005$; **Fig. 4a–c**) and between post-sleep retrieval-related hippocampal activation and overnight memory retention (all $P < 0.010$; **Fig. 4a–c**), the only significant path linking mPFC Aβ pathology to impaired memory retention was the sleep-dependent model (model 3), by way of the influence of mPFC Aβ on NREM SWA ($P = 0.017$; **Fig. 4c**). Thus, the association between mPFC Aβ pathology and diminished memory consolidation was significantly accounted for by the impairing influence of mPFC Aβ pathology on NREM SWA, resulting in a profile of greater overnight forgetting and persistent reliance on the hippocampus during next-day retrieval.

DISCUSSION

To the best of our knowledge, the current findings provide the first evidence that cortical Aβ pathology is associated with impaired generation of NREM slow wave oscillations that, in turn, predict the failure in long-term hippocampus-dependent memory consolidation. While it is important to recognize that these findings are cross-sectional and correlational, limiting causal claims, they nevertheless establish that the factors of Aβ and NREM sleep physiology and hippocampus-dependent memory are significantly and directionally interrelated. Thus, in addition to already established pathways associated with diminished cognitive function[2,3,5,6], Aβ may impair hippocampus-dependent memory in older adults through its impact on NREM SWA. Moreover, since sleep is a potentially modifiable factor, such findings raise the possibility that therapeutic sleep intervention may minimize the degree of cognitive decline associated with β-amyloid pathology in old age.

To date, age-related NREM sleep disruption has been described in older adult, mild cognitive impairment and Alzheimer's disease cohorts[13,16–18]. Moreover, subjective reports of poor quality sleep are associated with high Aβ burden in healthy older individuals[22], with reductions in SWS and REM sleep time associated with cerebrospinal fluid Aβ and tau protein levels in Alzheimer's disease patients[18]. These findings are supported by animal studies linking Aβ pathology to NREM sleep fragmentation[20]. The current study extends these reports by demonstrating that regionally specific aggregation of Aβ in mPFC is associated with the selective electrophysiological impairment of NREM SWA. Moreover, this sleep disruption subsequently predicts the impairment of hippocampal-neocortical memory transformation, further associated with significantly worse overnight memory retention.

Our findings further highlight specificity within this pathological interaction at two levels: anatomical and electrophysiological. Anatomically, the selective association between mPFC Aβ pathology (and not other common Aβ-accumulating regions) and diminished slow waves suggests that this region may be especially critical to the generation of such NREM sleep oscillations. Indeed, source localization analyses in healthy young adults have revealed slow wave generators in the same mPFC regions that commonly suffer early and extensive Aβ burden[2,4,15]. Electrophysiologically, the Aβ association with NREM SWA was specific to the frequency range of SWA between 0.6 and 1 Hz. This is of special relevance considering the two neurophysiologically distinct forms of NREM slow waves: the <1-Hz slow oscillation and the delta wave (1–4 Hz)[36,37]. While the mechanism underlying this frequency-specific association between mPFC Aβ and diminished slow waves (0.6–1 Hz) remains unknown, it is plausible that β-amyloid pathology impairs the generation and/or expression of slow oscillations through an impact on coordinated cortico-thalamic hyperpolarized down states and depolarized up states[36,37]. This may include the recognized reduction in synaptic NMDA receptor functioning by Aβ[38,39]—receptors that are also necessary for the generation of NREM slow oscillations (and not delta waves)[36–39]. In addition, or alternatively, Aβ may exacerbate age-related prefrontal atrophy owing to the neurotoxic effects of Aβ[2,3,38,39] or Aβ-coordinated spread of tau pathology through hippocampal-thalamic loops that interact with the thalamic reticular nucleus in the generation of NREM slow oscillations[3,5,40]. Importantly, all these hypotheses offer clear, testable predictions for future exploration in varied clinical and animal model systems.

In addition to Aβ being associated with diminished NREM sleep, a growing body of evidence suggests that NREM sleep disruption reciprocally promotes the buildup of Aβ. Interstitial Aβ levels in both humans and rodents rise during periods of wakefulness and fall during sleep[19]. Moreover, sleep deprivation increases Aβ plaque formation in rodent cortex[19] and alters cerebrospinal fluid Aβ levels in humans[41], whereas the presence of NREM sleep facilitates Aβ clearance[19,21]. Together with evidence linking Aβ pathology to NREM sleep disruption in rodents[20], the current findings describing a selective pathological associations with NREM SWA supports the interpretation of a bidirectional relationship between sleep and Aβ pathology. While remaining speculative, such an interpretation suggests a self-perpetuating cycle in which the initial emergence of Aβ impairs the generation of NREM sleep oscillations, which in turn results in wake-dependent increases in Aβ while diminishing the sleep-dependent clearance of Aβ[42]. As a result, Aβ buildup would accelerate, exacerbating the pathological cascade leading to Alzheimer's disease[3].

Beyond the association between Aβ burden and impaired NREM SWA, the current findings characterize a functional consequence of this association: impaired overnight consolidation of long-term memory. While prior evidence suggested that the strength of association between Aβ burden and memory retention in healthy older adults is only modest when memory is assessed immediately after encoding[1,3,6], the current findings indicate that this association becomes clear when the retention interval is delayed, and thus involves sleep-dependent memory processes. Consequently, our data suggest that one pathway linking cortical Aβ pathology to hippocampus-dependent long-term memory functioning is through the association between Aβ aggregation and disrupted NREM slow oscillations. Specifically, the data support a model in which the severity of Aβ aggregation in mPFC regions that generate NREM slow waves[15] predicts reductions in NREM slow waves 0.6–1 Hz. This reduction, in turn, is associated with diminished sleep-dependent memory consolidation and the persistent reliance (rather than the typical progressive independence[11,27,28,30]) of next-day memory retrieval on hippocampal activity. Indeed, results from the path analyses supported the hypothesis that the influence of mPFC Aβ on hippocampus-dependent memory consolidation is not direct but rather through its impact on NREM slow waves 0.6–1 Hz. These associations remained robust when adjusting for age, sex and atrophy.

These data in no way preclude the possibility that Aβ can influence memory independently of NREM slow waves or that other factors, such as atrophy or tau pathology, may influence memory independently of or depending on associations with NREM slow waves. While the statistical path analyses demonstrate significant interrelations between Aβ pathology, NREM sleep and hippocampus-dependent memory, they do not explain the influence of other, unmeasured factors, such as tau pathology, which may explain additional variance in age-related, sleep-dependent memory impairment. It is therefore necessary for future studies to employ models that examine multiple factors associated with age-related cognitive decline, to develop a more comprehensive account of how these factors interact with sleep and affect sleep-dependent memory. However, these findings do establish that one influence of Aβ pathology on hippocampus-dependent memory includes an impact on the cortical generation of NREM slow waves and the associated consolidation of sleep-dependent memory.

Building on this model, and more generally, our findings offer several clinical and public health considerations. First, should these associations prove to be causal in cognitively normal older adults and Alzheimer's disease cohorts, screening for and treating NREM slow wave sleep abnormalities may aid in reducing both the risk of developing the disease and the rate at which it progresses. Indeed, disordered sleep is recognized to carry an increased risk for cognitive decline and Alzheimer's disease[43,44], while superior sleep quality is associated with resilience to cognitive decline and a reduced risk of developing Alzheimer's disease[45]. Second, since associations between Aβ pathology and NREM sleep physiology are observed even in healthy older adults without clinically defined cognitive impairment, as well as in mild cognitive impairment and Alzheimer's disease cohorts[13,18], it is possible that disrupted SWA <1 Hz may represent a new biomarker in Alzheimer's disease, one that is detectable even before clinical symptoms emerge. Finally, these data offer the empirical foundations on which future work may determine whether Aβ-related sleep disruption plays a causal role in the progression of cognitive decline in neurodegenerative dementias. They further warrant the exploration of whether interventions that promote NREM SWA (in the 0.6–1 Hz frequency range) minimize the progression of neurodegeneration and the cognitive dysfunction associated with Aβ pathology.

METHODS

Methods and any associated references are available in the online version of the paper.

Note: Any Supplementary Information and Source Data files are available in the online version of the paper.

ACKNOWLEDGMENTS

We thank D. Baquirin, M. Belshe, M. Bhatter, M. Binod, S. Bowditch, C. Dang, J. Gupta, A. Hayenga, D. Holzman, A. Horn, E. Hur, J. Jeng, S. Kumar, J. Lindquist, C. Markeley, E. Mormino, M. Nicholas, S. Rashidi, M. Shonman, L. Zhang and A. Zhu for their assistance; A. Mander for his aid in task design; and M. Rubens and A. Gazzaley for use of their aging template brain. This work was supported by awards R01-AG031164 (M.P.W.), R01-AG034570 (W.J.J.) and F32-AG039170 (B.A.M.) from the US National Institutes of Health.

AUTHOR CONTRIBUTIONS

B.A.M. designed the study, conducted the experiments, analyzed the data and wrote the manuscript. S.M.M. aided in data analysis and manuscript preparation. J.W.V. aided in data collection, analysis and manuscript preparation. V.R. aided in data analysis and manuscript preparation. B.L. aided in study screening procedures and manuscript preparation. J.M.S. provided data analytic tools and aided in data analysis and manuscript preparation. S.A.-I. aided in study design and manuscript preparation. W.J.J. provided the subject pool and data analytic tools and aided in study design, PET data analysis and manuscript preparation. M.P.W. designed the study, aided in data analysis and wrote the manuscript.

COMPETING FINANCIAL INTERESTS

The authors declare no competing financial interests.

1. Boyle, P.A. *et al.* Much of late life cognitive decline is not due to common neurodegenerative pathologies. *Ann. Neurol.* **74**, 478–489 (2013).
2. Buckner, R.L. *et al.* Molecular, structural, and functional characterization of Alzheimer's disease: evidence for a relationship between default activity, amyloid, and memory. *J. Neurosci.* **25**, 7709–7717 (2005).
3. Jack, C.R. Jr. *et al.* Hypothetical model of dynamic biomarkers of the Alzheimer's pathological cascade. *Lancet Neurol.* **9**, 119–128 (2010).
4. Sepulcre, J., Sabuncu, M.R., Becker, A., Sperling, R. & Johnson, K.A. *In vivo* characterization of the early states of the amyloid-beta network. *Brain* **136**, 2239–2252 (2013).
5. Spires-Jones, T.L. & Hyman, B.T. The intersection of amyloid beta and tau at synapses in Alzheimer's disease. *Neuron* **82**, 756–771 (2014).
6. Mormino, E.C. *et al.* Episodic memory loss is related to hippocampal-mediated beta-amyloid deposition in elderly subjects. *Brain* **132**, 1310–1323 (2009).
7. Oh, H. & Jagust, W.J. Frontotemporal network connectivity during memory encoding is increased with aging and disrupted by beta-amyloid. *J. Neurosci.* **33**, 18425–18437 (2013).
8. Backhaus, J. *et al.* Midlife decline in declarative memory consolidation is correlated with a decline in slow wave sleep. *Learn. Mem.* **14**, 336–341 (2007).
9. Carrier, J. *et al.* Sleep slow wave changes during the middle years of life. *Eur. J. Neurosci.* **33**, 758–766 (2011).
10. Dijk, D.J., Beersma, D.G. & van den Hoofdakker, R.H. All night spectral analysis of EEG sleep in young adult and middle-aged male subjects. *Neurobiol. Aging* **10**, 677–682 (1989).
11. Mander, B.A. *et al.* Prefrontal atrophy, disrupted NREM slow waves, and impaired hippocampal-dependent memory in aging. *Nat. Neurosci.* **16**, 357–364 (2013).
12. Van Cauter, E., Leproult, R. & Plat, L. Age-related changes in slow wave sleep and REM sleep and relationship with growth hormone and cortisol levels in healthy men. *J. Am. Med. Assoc.* **284**, 861–868 (2000).
13. Westerberg, C.E. *et al.* Concurrent impairments in sleep and memory in amnestic mild cognitive impairment. *J. Int. Neuropsychol. Soc.* **18**, 490–500 (2012).
14. Marshall, L., Helgadottir, H., Molle, M. & Born, J. Boosting slow oscillations during sleep potentiates memory. *Nature* **444**, 610–613 (2006).
15. Murphy, M. *et al.* Source modeling sleep slow waves. *Proc. Natl. Acad. Sci. USA* **106**, 1608–1613 (2009).
16. Hita-Yañez, E., Atienza, M. & Cantero, J.L. Polysomnographic and subjective sleep markers of mild cognitive impairment. *Sleep* **36**, 1327–1334 (2013).
17. Prinz, P.N. *et al.* Sleep, EEG and mental function changes in senile dementia of the Alzheimer's type. *Neurobiol. Aging* **3**, 361–370 (1982).
18. Liguori, C. *et al.* Orexinergic system dysregulation, sleep impairment, and cognitive decline in Alzheimer disease. *JAMA Neurol.* **71**, 1498–1505 (2014).
19. Kang, J.E. *et al.* Amyloid-beta dynamics are regulated by orexin and the sleep-wake cycle. *Science* **326**, 1005–1007 (2009).
20. Roh, J.H. *et al.* Disruption of the sleep-wake cycle and diurnal fluctuation of beta-amyloid in mice with Alzheimer's disease pathology. *Sci. Transl. Med.* **4**, 150ra122 (2012).

21. Xie, L. *et al.* Sleep drives metabolite clearance from the adult brain. *Science* **342**, 373–377 (2013).
22. Spira, A.P. *et al.* Self-reported sleep and beta-amyloid deposition in community-dwelling older adults. *JAMA Neurol.* **70**, 1537–1543 (2013).
23. Chauvette, S., Seigneur, J. & Timofeev, I. Sleep oscillations in the thalamocortical system induce long-term neuronal plasticity. *Neuron* **75**, 1105–1113 (2012).
24. Kim, H. Neural activity that predicts subsequent memory and forgetting: a meta-analysis of 74 fMRI studies. *Neuroimage* **54**, 2446–2461 (2011).
25. Riedner, B.A. *et al.* Sleep homeostasis and cortical synchronization: III. A high-density EEG study of sleep slow waves in humans. *Sleep* **30**, 1643–1657 (2007).
26. Pascual-Marqui, R.D. Standardized low-resolution brain electromagnetic tomography (sLORETA): technical details. *Methods Find. Exp. Clin. Pharmacol.* **24** (suppl. D): 5–12 (2002).
27. Buzsáki, G. The hippocampo-neocortical dialogue. *Cereb. Cortex* **6**, 81–92 (1996).
28. Frankland, P.W. & Bontempi, B. The organization of recent and remote memories. *Nat. Rev. Neurosci.* **6**, 119–130 (2005).
29. Diekelmann, S. & Born, J. The memory function of sleep. *Nat. Rev. Neurosci.* **11**, 114–126 (2010).
30. Takashima, A. *et al.* Declarative memory consolidation in humans: a prospective functional magnetic resonance imaging study. *Proc. Natl. Acad. Sci. USA* **103**, 756–761 (2006).
31. Walker, M.P. The role of sleep in cognition and emotion. *Ann. NY Acad. Sci.* **1156**, 168–197 (2009).
32. Stage, F.K., Carter, H.C. & Nora, A. Path analysis: an introduction and analysis of a decade of research. *J. Educ. Res.* **98**, 5–12 (2004).
33. Bozdogan, H. Model selection and Akaike information criterion (Aic) — the general-theory and its analytical extensions. *Psychometrika* **52**, 345–370 (1987).
34. Kline, R.B. *Principles and Practice of Structural Equation Modeling* (Guilford, New York, 2011).
35. Raftery, A.E. Bayesian model selection in social research. *Sociol. Methodol.* **25**, 111–163 (1995).
36. Steriade, M., Contreras, D., Curro Dossi, R. & Nunez, A. The slow (< 1 Hz) oscillation in reticular thalamic and thalamocortical neurons: scenario of sleep rhythm generation in interacting thalamic and neocortical networks. *J. Neurosci.* **13**, 3284–3299 (1993).
37. Steriade, M., Nunez, A. & Amzica, F. A novel slow (< 1 Hz) oscillation of neocortical neurons *in vivo*: depolarizing and hyperpolarizing components. *J. Neurosci.* **13**, 3252–3265 (1993).
38. Kurup, P. *et al.* Abeta-mediated NMDA receptor endocytosis in Alzheimer's disease involves ubiquitination of the tyrosine phosphatase STEP61. *J. Neurosci.* **30**, 5948–5957 (2010).
39. Snyder, E.M. *et al.* Regulation of NMDA receptor trafficking by amyloid-beta. *Nat. Neurosci.* **8**, 1051–1058 (2005).
40. Cavdar, S. *et al.* The pathways connecting the hippocampal formation, the thalamic reuniens nucleus and the thalamic reticular nucleus in the rat. *J. Anat.* **212**, 249–256 (2008).
41. Ooms, S. *et al.* Effect of 1 night of total sleep deprivation on cerebrospinal fluid beta-amyloid 42 in healthy middle-aged men: a randomized clinical trial. *JAMA Neurol.* **71**, 971–977 (2014).
42. Ju, Y.E., Lucey, B.P. & Holtzman, D.M. Sleep and Alzheimer disease pathology—a bidirectional relationship. *Nat. Rev. Neurol.* **10**, 115–119 (2014).
43. Cricco, M., Simonsick, E.M. & Foley, D.J. The impact of insomnia on cognitive functioning in older adults. *J. Am. Geriatr. Soc.* **49**, 1185–1189 (2001).
44. Yaffe, K. *et al.* Sleep-disordered breathing, hypoxia, and risk of mild cognitive impairment and dementia in older women. *J. Am. Med. Assoc.* **306**, 613–619 (2011).
45. Lim, A.S. *et al.* Modification of the relationship of the apolipoprotein E epsilon4 allele to the risk of Alzheimer disease and neurofibrillary tangle density by sleep. *JAMA Neurol.* **70**, 1544–1551 (2013).
46. Brett, M., Anton, J.L., Valabregue, R. & Poline, J.B. Region of interest analysis using an SPM toolbox [abstract]. *NeuroImage* **16** (2, suppl. 1): 497 (2002).

ONLINE METHODS

Participants. Thirty healthy older adult participants were recruited, with 26 participants completing the study (18 female; mean ± s.d., 75.1 ± 3.5 years; **Table 1**). No statistical methods were used to predetermine sample sizes, but our sample sizes are similar to those reported in previous publications[6–8,11,47]. Data from ten of these participants were included in a previous publication[11]. These ten participants were selected for the present study, as they were the only participants with concurrently acquired PIB-PET data. The study was approved by the human studies committees at University of California, Berkeley and Lawrence Berkeley National Laboratories, with all participants providing written informed consent. Exclusion criteria included presence of neurologic, psychiatric or sleep disorders, current use of antidepressant or hypnotic medications, or being left-handed. Participants were free of depressive symptoms[48], and all scored >25 on the mini mental state exam[49]. Further, and in addition to neuroradiological assessments and medical interviews (compare refs. 11,47, obtained within 1 year of study entry), participants performed within 1.5 s.d. of their age-, sex- and education-matched control groups on tests of both episodic memory[50,51] and frontal function[52,53] (**Table 1**). Episodic memory task data were specifically excluded when below 2 s.d. of the mean across participants or when performing at chance levels. PIB DVR does not follow a normal distribution, and, unlike behavioral assessment, there are no numerical boundaries of the PIB DVR measure that render this metric without scientific or clinical relevance. Consequently, we did not use a PIB DVR exclusion threshold (within biological limits). Before study entry, participants underwent screening for sleep disorders with a polysomnography (PSG) recording night (described below) reviewed by a board-certified sleep medicine specialist (B.L.). Participants were excluded if they displayed evidence of a parasomnia or an apnea/hypopnea index ≥15 (ref. 54), with four participants being excluded owing to evidence of sleep apnea). All participants abstained from caffeine, alcohol and daytime naps for the 48-h before and during the study. Participants kept to their habitual sleep-wake rhythms and averaged 7–9-h of reported time in bed per night before study participation, verified by sleep logs (**Table 1**). The recording of sleep in the laboratory environment, as in the current study, is advantageous for a number of data acquisition and quality control reasons. However, it represents an important limitation considering that sleep amounts and efficiency are often greater in the home setting. While total sleep time and NREM SWS time often differ across these two contexts, the measure of NREM sleep spectral EEG power is highly consistent across nights within an individual in a variety of contexts, such that within-subject night-to-night variability is much smaller than between-subjects variability in NREM SWA[55,56]. This is of potential relevance to the current findings, since it was spectral NREM SWA that demonstrated associations with PIB and memory measures rather than any sleep stage metrics. Nevertheless, home PSG assessments will be necessary to provide a more ecologically valid exploration of the interaction between Aβ pathology, sleep and memory.

General experimental design. All participants underwent positron emission tomography (PET) scanning following [^{11}C]PIB injection. Within 1 year of PIB-PET scanning, participants then entered the lab in the evening and trained to criterion on a sleep-dependent episodic memory task (described below), followed by a short-delay (10 min) recognition test. Participants were then given an 8-h sleep opportunity, measured with PSG, starting at their habitual bed time (**Table 1**). Approximately 2 h after awakening, participants performed an event-related functional MRI (fMRI) scanning session while performing the long-delay (10-h) recognition test. PIB-PET data were acquired and analyzed separately (authors S.M.M. and J.W.V.) from all other data analyzed (author B.A.M.), thus ensuring that PSG, fMRI and memory data acquisition, preprocessing and analysis were conducted blind to participant Aβ status.

Episodic memory task. The word-pairs task[11] had an intentional encoding phase immediately followed by a training-to-criterion phase, which was then followed by a short-delay recognition test (10 min; 30 studied trials and 15 foil trials) and a long-delay recognition test (10 h, occurring in the MRI scanner 2 h after awakening; 90 studied trials and 45 foil trials).

As described previously[11], associative recognition memory was calculated by subtracting both the false alarm rate (FAR; proportion of foil words endorsed as "previously studied") and the lure rate (LR; proportion of previously studied words erroneously paired with the lure) from the hit rate (HR; proportion of previously studied words paired with the correct nonsense word)[11]. Episodic memory retention was subsequently calculated as the difference in short- and long-delay recognition memory performance (long-delay – short-delay)[11,57]. Two participants were excluded from analysis as outliers (memory performance more than 2 s.d. from the mean), and two participants had memory and fMRI data lost as a result of computer theft.

PET scanning and analysis. PIB-PET scans were collected within 1 year of sleep and memory assessment, as PIB distribution volume ratio (DVR) values change minimally within this duration[58,59]. Scanning was performed on 23 participants using a Siemens ECAT EXACT HR PET scanner and on 3 participants using a Siemens Biograph 6 PET/CT scanner in 3D acquisition mode after [^{11}C]PIB injection (approximately 15 mCi) into the antecubital vein. PIB DVR values have been shown to be highly comparable across these two scanners, having no effect on the global PIB measure[60]. Dynamic acquisition frames were obtained over 90 min, as reported[6,61], following transmission or CT scans for attenuation correction. PIB-PET data were reconstructed using an ordered subset expectation maximization algorithm with weighted attenuation, and images were smoothed using a 4-mm Gaussian kernel with scatter correction. Each image was evaluated for excessive motion and adequacy of statistical counts. PET image processing and analysis were performed using SPM8 to realign frames. Realigned PIB frames from the first 20 min of acquisition were averaged and used to guide coregistration of each individual's PIB-PET scan to their structural MRI scan. Logan graphical analysis was used to calculate voxel-wise distribution volume ratios (DVRs) with a cerebellar gray matter region of interest (ROI) used as a reference region, as described previously[6,61]. This analysis yielded a voxelwise DVR image for each participant. Targeting our mPFC hypothesis, the following Desikan-Killiany Atlas–derived[62] regions were used to construct our mPFC ROI: left and right hemisphere superior frontal regions, rostral and caudal anterior cingulate regions, and medial orbitofrontal region (**Fig. 1a**). In addition, occipital cortex (right and left hemisphere cuneus, lingual, pericalcarine and lateral occipital regions), temporal cortex (right and left hemisphere middle and superior temporal regions), parietal cortex (right and left hemisphere inferior and superior parietal, supramarginal gyrus and precuneus regions), and dorsolateral prefrontal cortex (dlPFC; right and left hemisphere rostral and caudal middle frontal, pars opercularis and pars triangularis regions) ROIs were used as control measures to determine specificity of mPFC Aβ effects. ROI DVR values were derived by calculating the mean of all voxel-wise DVR values within each ROI. To account for the non-normal distribution of Aβ in the population, DVR measures were normalized using the natural logarithm, as described previously[63–65].

MRI scanning. Scanning was performed on a Siemens Trio 3-T scanner equipped with a 32-channel head coil. Functional scans were acquired using a susceptibility-weighted, single-shot echo-planar imaging (EPI) method to image the regional distribution of the blood oxygenation level-dependent signal (time repetition (TR), 2,000 ms; time echo (TE), 23 ms; flip angle, 90°; FatSat, FOV 224 mm; matrix, 64 × 64; 37 3-mm slices with 0.3-mm slice gap; descending sequential acquisition] and using parallel imaging reconstruction (GRAPPA) with acceleration factor 2. Three functional runs were acquired (159 volumes, 5.3 min). Following functional scanning, two high-resolution T1-weighted anatomical images were acquired using a 3D MPRAGE protocol with the following parameters: TR, 1,900 ms; TE, 2.52 ms; flip angle, 9°; field of view (FOV), 256 mm; matrix, 256 × 256; slice thickness, 1.0 mm; 176 slices. Optimized voxel-based morphometry (VBM) was performed on coregistered mean MPRAGE images to examine gray matter volume in the same mPFC ROI used to extract mPFC PIB DVR values; VBM methods described in detail in ref. 11.

fMRI analysis. Functional MRI data were analyzed using SPM8 (Wellcome Department of Imaging Neuroscience; http://www.fil.ion.ucl.ac.uk/spm/software/), beginning with standardized preprocessing (realignment, slice timing correction and coregistration) and with normalization accomplished using a template derived from elderly brains as described previously[11,47].

Following preprocessing, retrieval trials were sorted into hits (correct word-nonsense word recognition), lures (selection of the incorrect, previously

doi:10.1038/nn.4035

studied, nonsense word), misses (incorrect selection of never-studied nonsense word or endorsement of word as "new"), correct rejections (novel words correctly endorsed as "new"), false alarms (novel words incorrectly endorsed as "studied") and omissions (trials with no subject response)[11], with each trial modeled using a canonical hemodynamic response function. To generate a validated contrast for retrieval-related activity, hit events were contrasted with correct rejection events (hits – correct rejections)[11]. Individual activation maps were then taken to a second-level random effects analysis to examine retrieval-related activation negatively associated with NREM SWA and overnight memory retention measures. Activations were assessed at a voxel level of $P < 0.05$ family-wise error[66] corrected for multiple comparisons within an a priori hippocampal region of interest (ROI; 8 mm sphere [$x = -22$, $y = -14$, $z = -12$][24] in Talairach space and [$x = -23$, $y = -15$, $z = -16$] after MNI conversion[67]), further inclusively masked using an anatomical hippocampus ROI. To determine associations between hippocampus activation and other variables of interest, the cluster average of significant voxels was extracted using Marsbar[46].

Sleep monitoring and EEG analysis. PSG on the night of the experiment was recorded using a Grass Technologies Comet XL system (Astro-Med, Inc., West Warwick, RI), including 19-channel electroencephalography (EEG) placed using the 10–20 system, electrooculography (EOG) recorded at the right and left outer canthi (right superior; left inferior) and electromyography (EMG). Reference electrodes were recorded at both the left and right mastoid (A1, A2). Data were digitized at 400 Hz and stored unfiltered (recovered frequency range of 0.1–100 Hz), except for a 60-Hz notch filter. Sleep was scored using standard criteria[68]. Sleep monitoring on the screening night was recorded using a Grass Technologies AURA PSG Ambulatory system (Astro-Med, Inc., West Warwick, RI) and additionally included nasal and oral airflow sensors, abdominal and chest belts, and pulse oximetry.

EEG data from the experimental night were imported into EEGLAB (http://sccn.ucsd.edu/eeglab/) and epoched into 5 s bins. Epochs containing artifacts were manually rejected by a trained scorer (B.A.M.), and the remaining epochs were filtered between 0.4 and 50 Hz (645 ± 80 epochs per participant with 4.6% ± 2.1% of epochs rejected). A fast Fourier transform (FFT) was then applied to the filtered EEG signal at 5-s intervals with 50% overlap and employing Hanning windowing. Analyses in the current report focused, a priori, on slow wave activity (SWA), defined as relative spectral power between 0.6 and 4.6 Hz during slow wave sleep (NREM stages 3 and 4)[10,11]. Spectral power was subdivided into two bins for analysis (0.6–1 Hz and 1–4 Hz), to examine the impact of Aβ on SWA frequencies particularly relevant to memory functions[14,23]. A single summary proportional measure was also derived by dividing the spectral power between 0.6 and 1 Hz by the sum of spectral power between 0.6 and 4 μHz, to determine the relative dominance of memory-relevant slow waves. Furthermore, because of our a priori focus on mPFC, SWA measures at FZ and CZ EEG derivations were averaged and used as a measure of mPFC SWA (**Fig. 1b**). To ascertain topographic specificity of effects, SWA measures at F3, F4, F7 and F8 EEG derivations were averaged and used as a measure of dlPFC SWA; SWA measures at P3, P4 and PZ EEG derivations were averaged and used as a measure of parietal SWA; SWA measures at T3, T4, T5 and T6 EEG derivations were averaged and used as a measure of temporal SWA; and SWA measures at O1 and O2 EEG derivations were averaged and used as a measure of occipital SWA.

Slow wave detection and source analysis were performed to calculate the impact of mPFC Aβ on slow wave density and to determine whether memory-relevant FZ and CZ–measured slow waves (0.6–1 Hz) have an mPFC source (**Fig. 1b** and **Supplementary Fig. 2**). EEG data were filtered between 0.5–4 Hz, and individual slow waves were detected using a validated algorithm[25]. Standardized low-resolution brain electromagnetic tomography (sLORETA) was employed[26] as previously described[69,70]. In short, this method calculates current density sources using a discrete, three-dimensionally distributed, linear minimum norm solution to the forward problem. Computations are made using a head model based on the MNI152 template[71]. Prior to sLORETA analysis, EEG preprocessing was conducted in MATLAB using the EEGLAB toolbox. For each participant, the filtered (0.5 Hz–4 Hz), artifact-rejected EEG was event-marked separately for detected slow wave (0.6–1 Hz) midpoints in the FZ and CZ derivations. EEG was then epoched around each detected slow wave midpoint (±100 ms). Slow wave epochs were then averaged and exported separately for CZ and FZ–detected slow waves. sLORETA analyses of slow wave epochs were carried out using the freeware sLORETA utilities (http://www.uzh.ch/keyinst/loreta.htm), consistent with previous source analysis examinations[69,70]. Prior to current density source calculation, all electrode derivations were registered and transformed into 3D MNI space, yielding a spatial transformation matrix. Current density source maps were then derived for each participant separately for CZ and FZ time-locked EEG averages. CZ and FZ source maps were then averaged within each participant, with CZ-FZ averaged source maps then averaged across participants to generate a grand mean average source image for memory-relevant CZ and FZ slow waves (**Supplementary Fig. 2**).

Statistical analysis. Two-way repeated measures ANCOVA models were used to determine the influence of PIB-PET measures on NREM slow wave measures, with PIB-PET DVR measures as a between-subjects covariate and frequency (0.6–1 Hz or 1–4 Hz) as a within-subjects factor. Associations between PIB DVR measures, sleep measures, hippocampal activation and episodic memory retention were assessed using regression models. Normality was formally tested, and all variables exhibited the skewness and kurtosis of a normal distribution except PIB-PET DVR measures, which exhibited a normal kurtosis but a right-skewed distribution. Since PIB-PET DVR measures followed a right skewed non-normal distribution, PIB DVR values were natural logarithm–transformed before analysis and regressions were further affirmed with follow-up nonparametric Kendall's τ correlations. Analyses were completed using SPSS version 22.0 (SPSS, Inc., Chicago, IL).

To determine whether mPFC Aβ statistically influenced hippocampal-dependent episodic memory retention through mPFC NREM SWA, path analyses were performed using a structural equation modeling framework[32,34] in Amos version 22 (IBM Corp., Armonk, NY). This multivariate modeling technique calculates the path coefficients—that is, coupling between model variables, given a specified model. Path coefficients reflect the direct and proportional influence of one variable on another while controlling for other variables in the model. Three hypothesized models were specified with an equal number of paths. These models were then compared to each other and to saturation and independence models. The first model allowed Aβ to directly affect memory retention independently of NREM SWA. The second model allowed Aβ to affect memory retention independently of NREM SWA, but this time indirectly through its effects on hippocampal activation. The third model instead required Aβ to affect memory retention solely through its influence on NREM SWA. Three validated metrics were used to compare model fits: BIC (Bayesian information criterion), RMR (root-mean-squared residual) and GFI (goodness-of-fit index)[33–35]. Models with RMR near 0 and GFI above 0.9 were considered sufficient model fits[34]. The model with the lowest BIC value was considered the best model, with a difference of >10 suggesting large model differences, a difference of 6–10 suggesting medium model differences, and a difference of 2–6 suggesting small model differences[35]. Within the best model, individual path coefficients were then examined for significance.

A **Supplementary Methods Checklist** is available.

47. Mander, B.A. *et al.* Impaired prefrontal sleep spindle regulation of hippocampal-dependent learning in older adults. *Cereb. Cortex* **24**, 3301–3309 (2014).
48. Yesavage, J.A. *et al.* Development and validation of a geriatric depression screening scale: a preliminary report. *J. Psychiatr. Res.* **17**, 37–49 (1982–1983).
49. Folstein, M.F., Folstein, S.E. & McHugh, P.R. "Mini-mental state". A practical method for grading the cognitive state of patients for the clinician. *J. Psychiatr. Res.* **12**, 189–198 (1975).
50. Delis, D., Kramer, J., Kaplan, E. & Ober, B. *California Verbal Learning Test* (The Psychological Corporation, San Antonio, Texas, USA, 2000).
51. Wechsler, D. *Wechsler Memory Scale—Revised* (The Psychological Corporation, San Antonio, Texas, USA, 1987).
52. Reitan, R.M. Validity of the trail-making test as an indication of organic brain damage. *Percept. Mot. Skills* **8**, 271–276 (1958).
53. Zec, R.F. The Stroop color-word test: a paradigm for procedural learning. *Arch. Clin. Neuropsychol.* **1**, 274–275 (1986).
54. Young, T., Peppard, P.E. & Gottlieb, D.J. Epidemiology of obstructive sleep apnea: a population health perspective. *Am. J. Respir. Crit. Care Med.* **165**, 1217–1239 (2002).
55. Tan, X., Campbell, I.G. & Feinberg, I. Internight reliability and benchmark values for computer analyses of non-rapid eye movement (NREM) and REM EEG in normal young adult and elderly subjects. *Clin. Neurophysiol.* **112**, 1540–1552 (2001).

56. Zheng, H. *et al.* Sources of variability in epidemiological studies of sleep using repeated nights of in-home polysomnography: SWAN Sleep Study. *J. Clin. Sleep Med.* **8**, 87–96 (2012).
57. Cohen, D.A. & Robertson, E.M. Preventing interference between different memory tasks. *Nat. Neurosci.* **14**, 953–955 (2011).
58. Jack, C.R. Jr. *et al.* Brain beta-amyloid load approaches a plateau. *Neurology* **80**, 890–896 (2013).
59. Villemagne, V.L. *et al.* Amyloid beta deposition, neurodegeneration, and cognitive decline in sporadic Alzheimer's disease: a prospective cohort study. *Lancet Neurol.* **12**, 357–367 (2013).
60. Elman, J.A. *et al.* Neural compensation in older people with brain amyloid-beta deposition. *Nat. Neurosci.* **17**, 1316–1318 (2014).
61. Oh, H., Madison, C., Haight, T.J., Markley, C. & Jagust, W.J. Effects of age and beta-amyloid on cognitive changes in normal elderly people. *Neurobiol. Aging* **33**, 2746–2755 (2012).
62. Desikan, R.S. *et al.* An automated labeling system for subdividing the human cerebral cortex on MRI scans into gyral based regions of interest. *Neuroimage* **31**, 968–980 (2006).
63. Bradshaw, E.M. *et al.* CD33 Alzheimer's disease locus: altered monocyte function and amyloid biology. *Nat. Neurosci.* **16**, 848–850 (2013).
64. Hedden, T. *et al.* Cognitive profile of amyloid burden and white matter hyperintensities in cognitively normal older adults. *J. Neurosci.* **32**, 16233–16242 (2012).
65. Hedden, T. *et al.* Failure to modulate attentional control in advanced aging linked to white matter pathology. *Cereb. Cortex* **22**, 1038–1051 (2012).
66. Lieberman, M.D. & Cunningham, W.A. Type I and type II error concerns in fMRI research: re-balancing the scale. *Soc. Cogn. Affect. Neurosci.* **4**, 423–428 (2009).
67. Lancaster, J.L. *et al.* Bias between MNI and Talairach coordinates analyzed using the ICBM-152 brain template. *Hum. Brain Mapp.* **28**, 1194–1205 (2007).
68. Rechtschaffen, A. & Kales, A. *A Manual of Standardized Terminology, Techniques and Scoring: System of Sleep Stages in Human Subjects* (UCLA Brain Information Services, Los Angeles, 1968).
69. Mander, B.A., Santhanam, S., Saletin, J.M. & Walker, M.P. Wake deterioration and sleep restoration of human learning. *Curr. Biol.* **21**, R183–R184 (2011).
70. Saletin, J.M., van der Helm, E. & Walker, M.P. Structural brain correlates of human sleep oscillations. *Neuroimage* **83**, 658–668 (2013).
71. Mazziotta, J. *et al.* A probabilistic atlas and reference system for the human brain: International Consortium for Brain Mapping (ICBM). *Phil. Trans. R. Soc. Lond. B* **356**, 1293–1322 (2001).

doi:10.1038/nn.4035